

P4.5 Three-Dimensional Mosaic of the Eddy Dissipation Rate Fields from WSR-88Ds

Ming Fang* and Jian Zhang

Cooperative Institute of Mesoscale Meteorological Studies,
University of Oklahoma, Norman, Oklahoma

John K. Williams and Jason A. Craig

National Center for Atmospheric Research, Boulder, Colorado

1. INTRODUCTION

A national 3-D mosaic of in-cloud turbulence, represented as Eddy Dissipation Rate (EDR), is being developed and prototyped through collaboration between the National Center for Atmospheric Research (NCAR) and NOAA's National Severe Storms Lab (NSSL) under the auspices of the FAA Aviation Weather Research Program's Turbulence and Advanced Weather Radar Techniques (AWRT) Research Teams (RTs). The EDR field is an indicator of in-cloud turbulence intensity derived from WSR-88Ds' spectrum width data by the NEXRAD Turbulence Detection Algorithm (NTDA, Williams et al. 2006), which was developed at NCAR by the Turbulence RT. The NTDA software has been delivered to the National Weather Service Radar Operations Center and will be implemented operationally on all WSR-88Ds beginning in the spring of 2008, providing EDR and the associated confidence field, called EDC, as polar-grid Level III data for each radar elevation tilt. A national 3-D mosaic of the EDR field will provide a high-resolution, rapid update, in-cloud turbulence product for use in aviation safety decision support processes. In particular, the Turbulence RT plans to incorporate it into a new rapid-update version of the Graphical Turbulence Guidance product, which will directly address convective turbulence for the first time.

An initial 3-D EDR mosaic capability has been developed using NTDA data from 20 radars covering the Chicago to Washington DC region. The NTDA data are generated at NCAR (see Craig et al. 2008) and transferred to NSSL in real-time. A mosaic scheme previously developed by the AWRT RT for creating 3-D reflectivity mosaics (Zhang et al. 2005) was used as a starting point, and a number of adjustments were made to accommodate differences between the physical characteristics associated with EDR and reflectivity fields. In addition, the EDC data, which reflect the estimated quality of the associated EDR, should be incorporated into the 3-D mosaic weighting scheme,

whereas no comparable confidence field exists for the reflectivity data. Presented in this paper are some preliminary results from the initial 3-D EDR and EDC mosaics. Further adjustments and enhancements to the system are still underway.

2. THE REAL-TIME TURBULENCE MOSAIC SYSTEM (RTTMS)

Real-time EDR and EDR confidence (EDC) fields for 20 radars (Table 1) are currently being transferred from NCAR to NSSL through FTP in real-time. The RTTMS ingests these real-time single radar, single elevation tilt data fields and generates 3-D EDR and EDC mosaics on a regional domain (Fig. 1). The northwest corner of the RTTMS domain is at (44.1N, -96.7W), and the southeast corner is (33.6N, -74.6W). The horizontal resolution of the RTTMS grid is 0.02° latitude \times 0.02° longitude ($\sim 2\text{km} \times 2\text{km}$), and there are 31 vertical levels (Table 2) in the 3-D turbulence mosaic grid.

Table 1 List of radars from which EDR and EDC fields are transferred from NCAR to NSSL in real-time.

Radar ID	Lat ($^\circ$ N)	Lon ($^\circ$ W)		Radar ID	Lat ($^\circ$ N)	Lon ($^\circ$ W)
KAKQ	36.984	-77.007		KIWX	41.359	-85.700
KCCX	40.923	-78.004		KJKL	37.591	-83.313
KCLE	41.413	-81.860		KLOT	41.604	-88.085
KDMX	41.731	-93.723		KLSX	38.699	-90.683
KDVN	41.612	-90.581		KLVX	37.975	-85.944
KEAX	38.810	-94.264		KLWX	38.975	-77.478
KFCX	37.024	-80.274		KPAH	37.068	-88.772
KILN	39.420	-83.822		KRLX	38.311	-81.723
KILX	40.150	-89.337		KSGF	37.235	-93.400
KIND	39.708	-86.280		KVWX	38.260	-87.724

* Corresponding author address: Ming Fang, 120 David L Boren Blvd., Norman, OK 73072; email: ming.fang@noaa.gov

their native grids in spherical coordinates to the three-dimensional mosaic grid in a Cartesian coordinate system. The interpolation and mosaicking schemes are described in the following section.

Module 4 converts the 3-D mosaicked squared EDR field back to the cubed root eddy dissipation rate and outputs the final 3-D EDR and EDC mosaic grids.

The initial version of RTTMS has been running in real-time at NSSL since September 29, 2007. In the system, a main program calls these four models and runs in real-time on clock, currently at every 5 min.

The update cycle for the 3-D turbulence mosaic is eventually expected to be reduced to every 2.5 min, and the NetCDF files will be replaced with NEXRAD Level III NTDA data once the operational NTDA products are available from the NEXRAD ORPG (Open Radar Product Generator).

3. INTERPOLATION AND MOSAICKING ALGORITHMS

The 3-D radar reflectivity mosaic scheme developed by Zhang et al. (2005) was adapted for the interpolation and mosaicking of the turbulence field. There are three interpolation schemes for transforming single radar data fields from spherical coordinates to a 3-D regular grid in Cartesian coordinates. The first scheme, Nearest Neighbor mapping, assigns the value from the nearest radar bin (i.e., measurement location) to each Cartesian grid cell. The distance between a radar bin and a given grid cell is calculated from the center of the radar bin to the grid cell's center.

The second scheme, Vertical Interpolation, applies a linear interpolation in the elevation (vertical) direction while taking the nearest neighbor approach in azimuth and range directions. The vertical interpolation is performed between all pairs of adjacent tilts.

The third scheme, Vertical and Horizontal Interpolation, is the vertical interpolation approach combined with a horizontal interpolation. The horizontal interpolation is only applied between adjacent tilts within certain range limits, where horizontal distance between centers of the adjacent tilts are less than a user-defined threshold (default value = 25 km).

Once single radar fields from each radar are interpolated to the Cartesian grid, each grid cell covered by multiple radars is examined. The final

mosaicked value is computed from a weighted mean of the multiple radar values using the weighting function of $w = \exp\left[-d^2/D_0\right]$ for each. Here d is the distance from the grid cell to a given radar site, and D_0 is a constant which is set to $(50 \text{ km})^2$.

4. CASE STUDY

A playback version of the RTTMS has also been developed for rerun of historical events. Using the playback system, 3-D turbulence mosaic fields for two squall line cases were analyzed.

Fig. 3 shows example 3-D EDR and EDC mosaic fields from the RTTMS on October 1, 2007. The vertical interpolation scheme was used to obtain the results. A squall line associated with a cold front runs north-south from western Wisconsin to the northeast corner of Oklahoma (Fig.3a). The large values in the EDR and EDC mosaic fields (Figs.3b and 3c) corresponded well with the most intensive reflectivity in the squall line. There were also some notable differences between the turbulence and the reflectivity fields. For instance, there were some circle-shaped gaps in the mosaicked EDR and associated confidence fields (Figs. 3b and 3c). These gaps are due to factors such as the gaps between adjacent tilts, the insufficient signal in the 2nd trip echo recovery procedure and the limited coverage (230 km) of the WSR-88D's Doppler fields. Mitigating these artifacts is a challenge because a large-scale smoothing/gap-filling that works well for the radar reflectivity would not be appropriate for EDR because of the typically small scales of turbulence patches. Additional radars could provide better coverage and fill in some of the gaps (e.g., by running a version of the NTDA on TDWR radars), and use of a scan strategy with more sweeps and smaller elevation increments would be very helpful as well. In addition, the Turbulence RT has proposed a new spectrum width estimator for NEXRADs that should produce usable spectrum widths in regions of lower SNR than the current estimator (Meymaris and Williams 2007), and is also working on a second version of the NTDA that should provide improved coverage, particularly at lower altitudes.



Fig. 3a. Composite reflectivity from the RTMS valid at 01:00UTC on 10/01/2007.

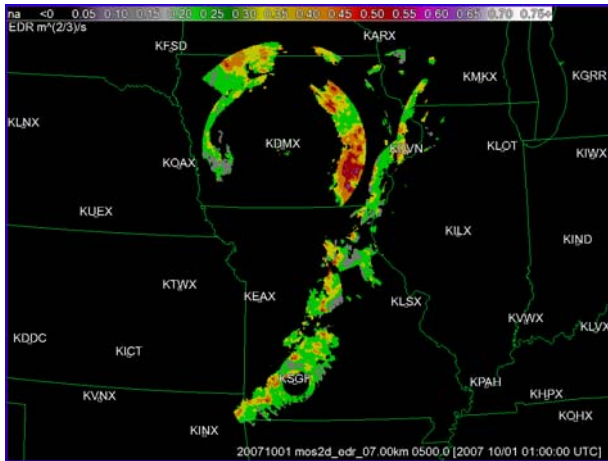


Fig. 3b. Horizontal cross section of the EDR mosaic field at 7 km (MSL) valid at 01:00UTC on 10/01/2007.

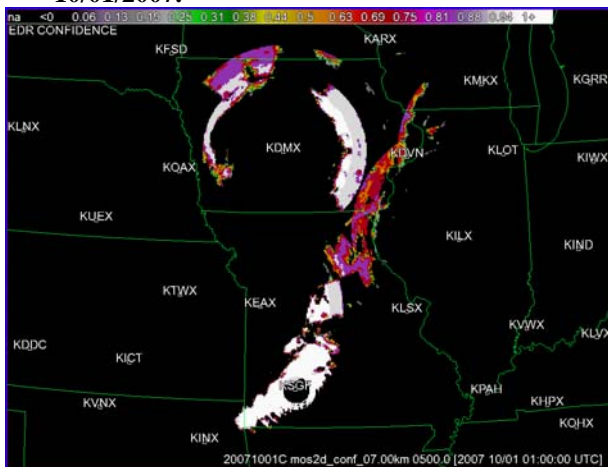


Fig. 3c. Horizontal cross section of the EDC mosaic field at 7 km (MSL) valid at 01:00UTC on 10/01/2007.

Fig. 4 shows example results from a severe storm event that occurred on August 24, 2007. The relatively large values of EDR (Fig.4b) on the squall line correlated well with the strong convection (e.g., areas with reflectivity higher than 40 dBZ, Fig.5a). For the data displayed in Figs.4b and 4c, the Nearest Neighbor interpolation scheme was used to remap the single radar EDR and EDC from spherical system onto the three dimensional Cartesian grids. There are circle-shaped “cone of silence” regions around radars (Figs.4b and 4c); these holes appear more prominent in the EDR than the reflectivity field because they are less likely to be filled in using data from adjacent radars. Figs. 5 and 6 show mosaicked EDR fields using the Vertical Interpolation and the Vertical and Horizontal Interpolation schemes, respectively. Comparing Fig. 5 with Fig. 4b one can see that the Vertical Interpolation alleviated the circle-shaped “ring” artifacts around KSGF and KLSX radars significantly. The Vertical and Horizontal Interpolation did an even better job (Fig. 6).

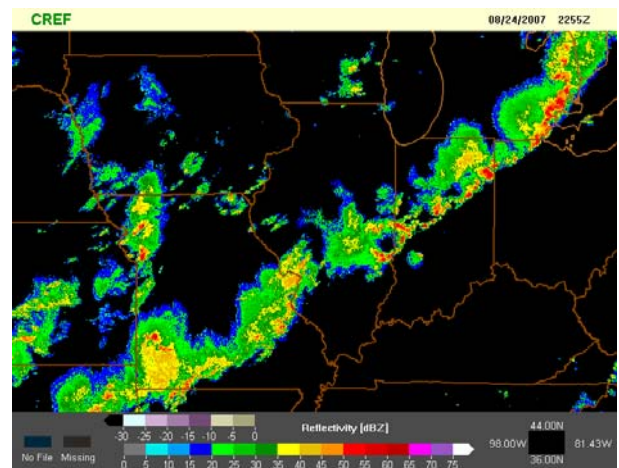


Fig. 4a. Composite reflectivity for a squall line event that occurred on 24 August 2007. The images are valid at 22:55UTC.

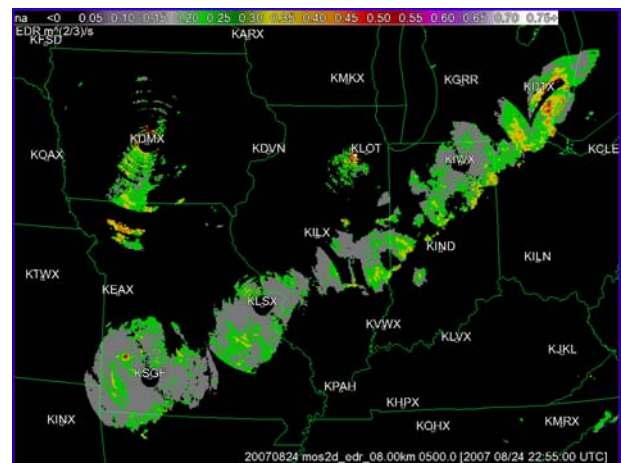


Fig. 4b. The EDR mosaic field at 8 km (MSL) height corresponding to Fig 4a. The Nearest-neighbor algorithm was used to remap the single radar data from spherical coordinates to the three dimensional Cartesian grids.

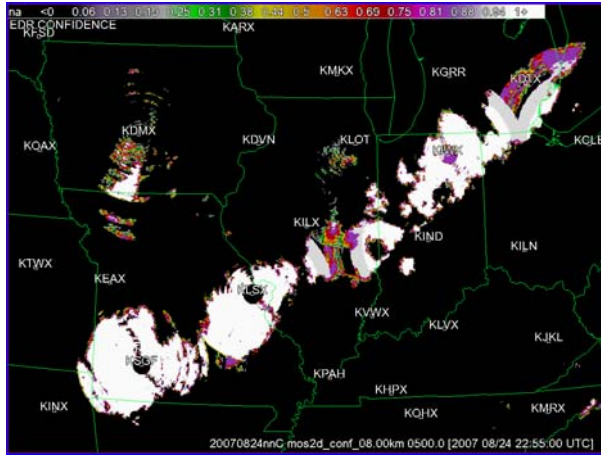


Fig. 4c. Same as in Fig.4b except showing the EDC field.



Fig. 5. Same as Fig. 4b, but with the Vertical Interpolation scheme.

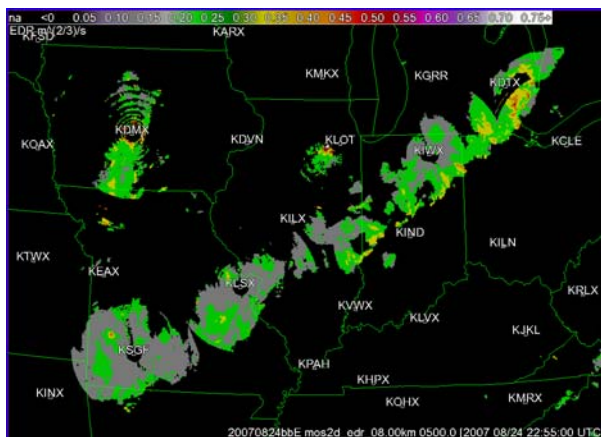


Fig. 6. Same as Fig. 4b, but with the Vertical and Horizontal Interpolation scheme.

5. FUTURE WORK

In the future, we will use *in situ* turbulence reports from commercial airplanes (Cornman et al. 2004) to evaluate the accuracy of the turbulence mosaic grids, and to quantitatively compare alternative mosaic schemes based on both their accuracy and coverage. In particular, we will continue to evaluate the algorithms that remap single radar data from spherical coordinates to three-dimensional Cartesian grids as well as the weighting function for mosaicking EDR and EDC fields from multiple radars. We will also explore ways of using the EDC field in the weighting scheme for the 3-D EDR mosaic.

6. ACKNOWLEDGEMENT

This research is in response to requirements and funding by the Federal Aviation Administration (FAA). The views expressed are those of the authors and do not necessarily represent the official policy or position of the FAA.

7. REFERENCES

- Cornman, L. B. and R. K. Goodrich, 1996: The detection of atmospheric turbulence using Doppler radars. *Preprints, Workshop on Wind Shear and Wind Shear Alert Systems*, Oklahoma City, Oklahoma.
- Cornman, L. B., G. Meymaris and M. Limber, 2004: An update on the FAA Aviation Weather Research Program's *in situ* turbulence measurement and reporting system. *11th AMS Conference on Aviation, Range, and Aerospace Meteorology*, Hyannis, MA, 4.3.
- Craig, J. A. and J. K. Williams, G. Blackburn, S. Linden, and R. Stone, 2008: Remote detection and real-time alerting for in-cloud turbulence. *13th AMS Conference on Aviation, Range and Aerospace Meteorology*, New Orleans, LA, 9.4.
- Labitt, M., 1981: Coordinated radar and aircraft observations of turbulence. Proj. Rrp. ATC 108. M.I.T., Lincoln Lab., Cambridge.
- Meymaris, G. and J. K. Williams, 2007: Spectrum width estimators for the NEXRAD ORDA: evaluation and recommendation. *AMS 23rd*

Conference on Interactive Information Processing Systems, San Antonio, TX, 5B.5.

Williams, J. K., L. B. Cornman, J. Yee, S. G. Carson, G. Blackburn and J. Craig, 2006: NEXRAD detection of hazardous turbulence. *44th AIAA aerospace sciences meeting and exhibit*, Reno, Nevada, AIAA 2006-0076.

Zhang, J., K. Howard, and J. J. Gourley, 2005: Constructing Three-Dimensional Multiple-Radar Reflectivity Mosaics: Examples of Convective Storms and Stratiform Rain Echoes. *J. Atmos. Oceanic Technol.*, **22**, 30–42.